Evaluation of Anisotropy using Knoop indenter

A.R.S.M

2019. 05. 13.

Material Reliability
& Forensic Safety Lab.

Why use 3D printing

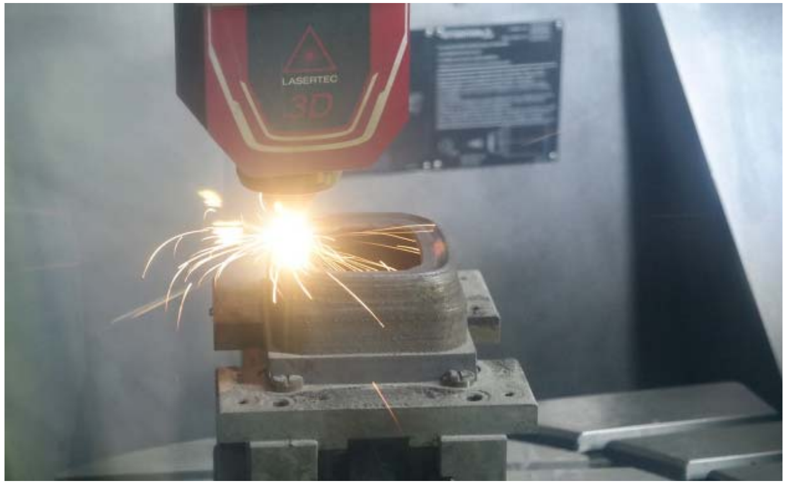

3D Printing Technique →

Cost Reduction

Lightweight

Efficiency Improvement

Anisotropic issues

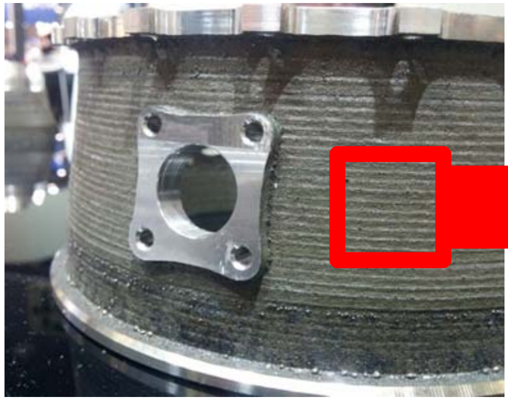

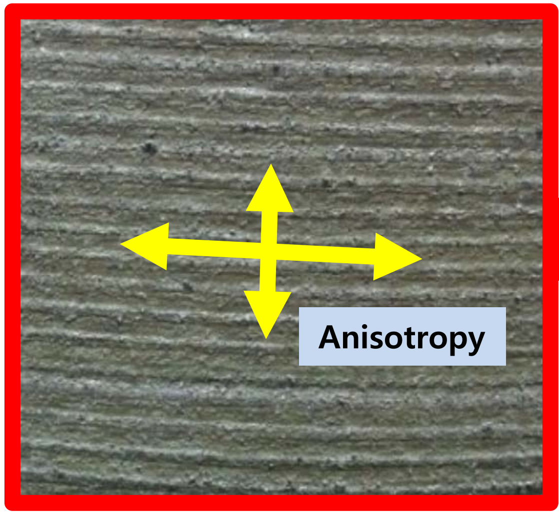

Failure !!

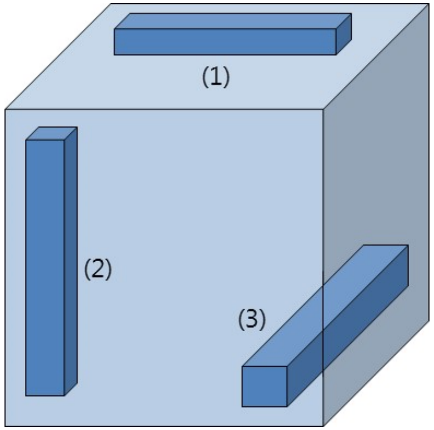

Sampling

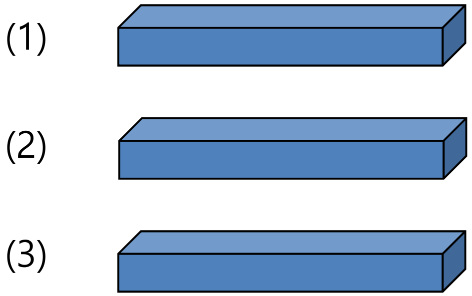

Elastic modulus (E)

Poisson's ratio (ν)

⋮

$$E_{(1)} = E_{(2)} = E_{(3)}$$
$$\nu_{(1)} = \nu_{(2)} = \nu_{(3)}$$

=> **Isotropic material**

$$E_{(1)} \neq E_{(2)} \neq E_{(3)}$$
$$\nu_{(1)} \neq \nu_{(2)} \neq \nu_{(3)}$$

=> **Anisotropic material**

Microstructures of N, R, T plane depending on reduction rate

Optical micrographs

	N plane	T plane	R plane

Reduction Rate [%]

0%

20%

40%

60%

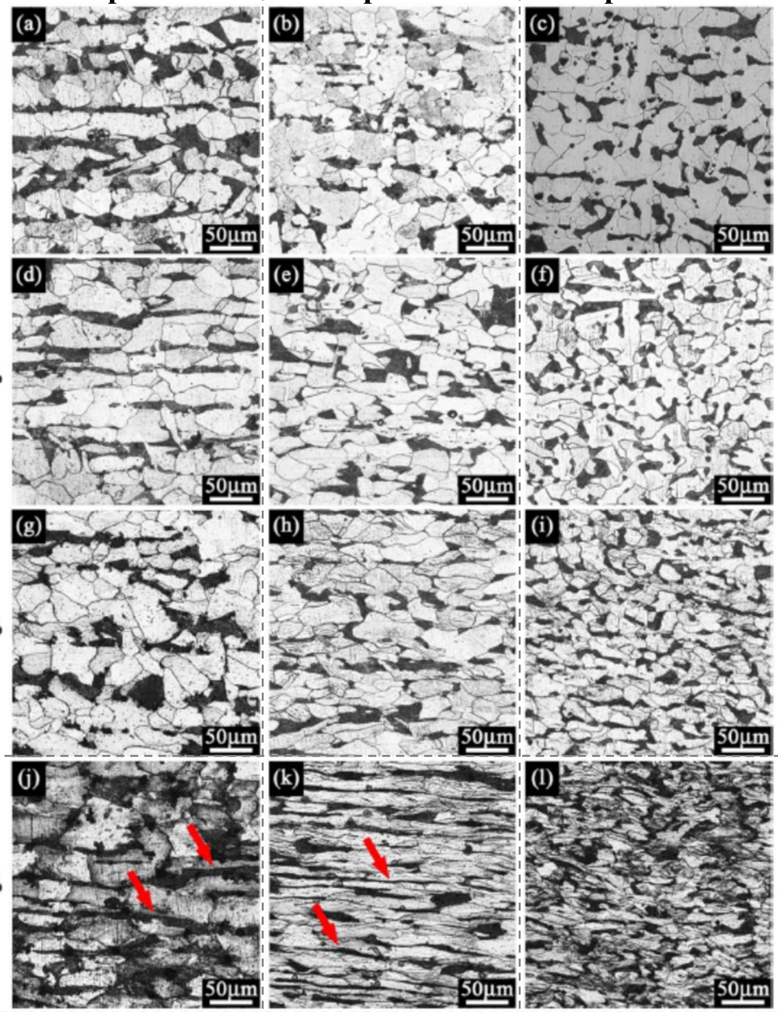

N plane	T plane	R plane
- Slight elongated grains	- Severe deformation - Elongated grains	- Slight elongated grains

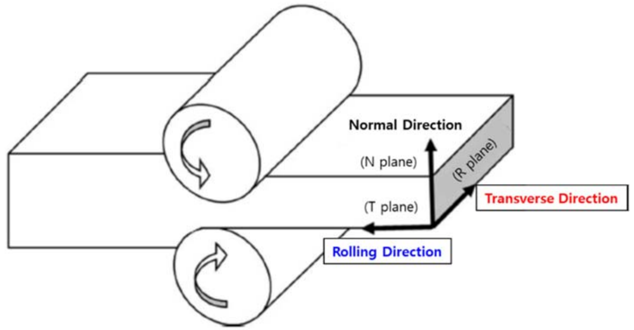

EBSD-OIM micrographs (60%)

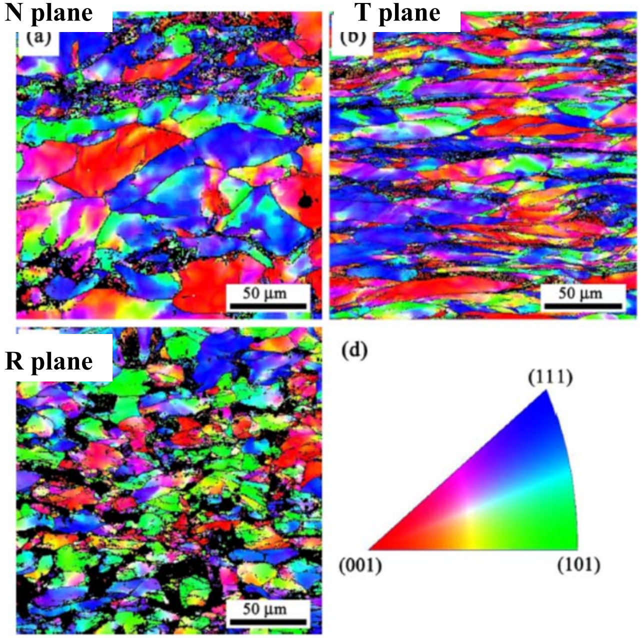

- N plane : Slight elongated grains
- T plane : Elongated grains along the rolling direction
- R plane : More or less equiaxed grains

S. Choudhary, V. Nanda, S. Shekhar, A. Garg, and K. Mondal, Effect of Microstructural Anisotropy on the Electrochemical Behavior of Rolled Mild Steel, JMEPEG (2017) 26:185–194

Grains of N, R, T plane depending on reduction rate

Schematic grain shape

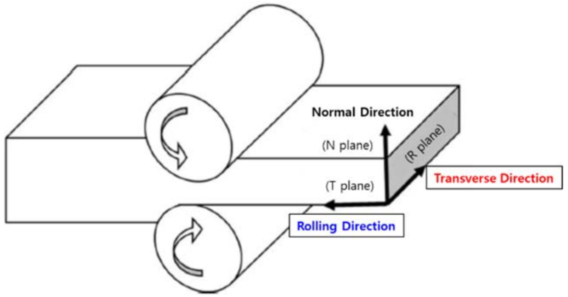

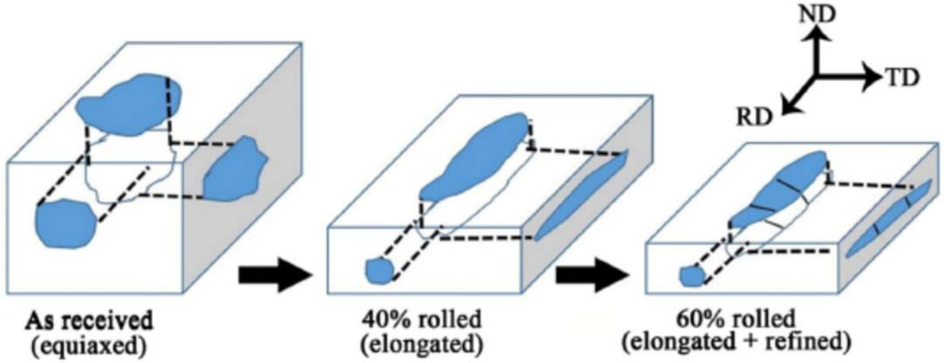

Yield Strength

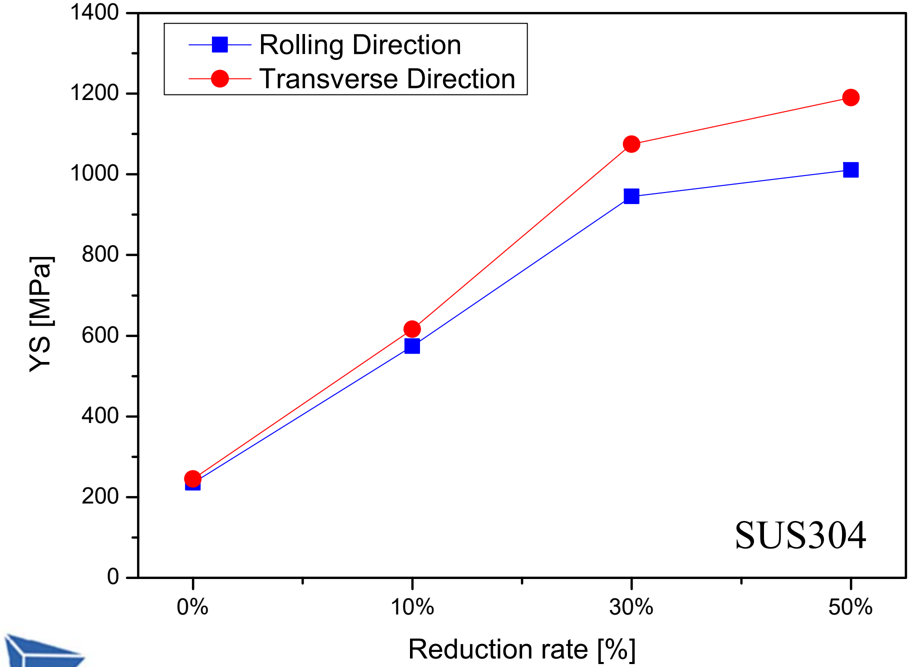

Tensile Strength

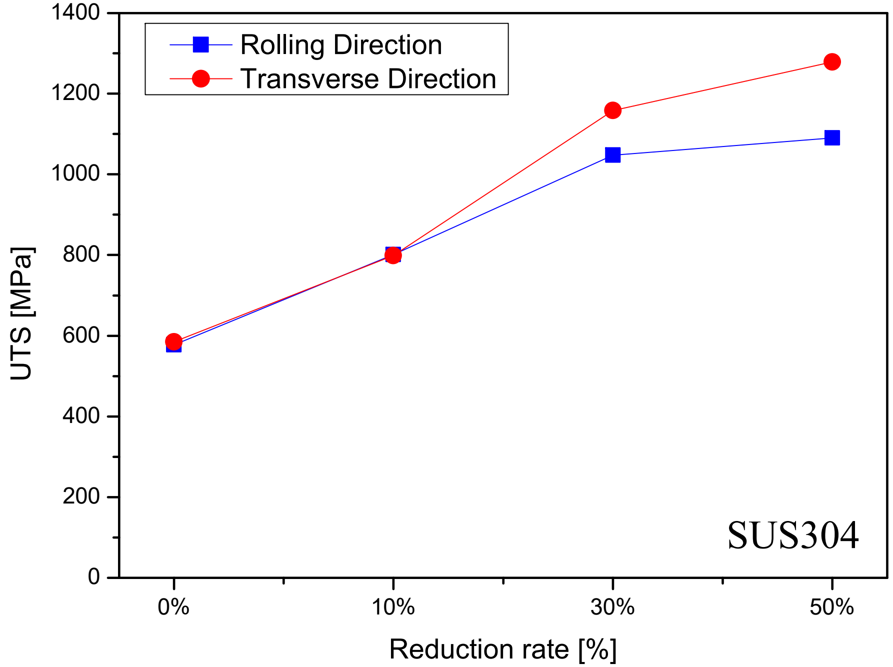

Separation of load difference with stress directions

Knoop indenter

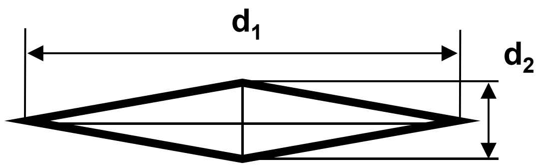

$d_1 : d_2 \cong 7:1$

Stress-free Uni-axial stress

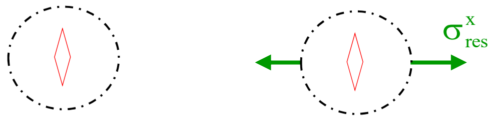

Comparison of indentation curves

$$\Delta L \approx \alpha_{\perp} \sigma^x_{res}$$

conversion factor in **normal** direction

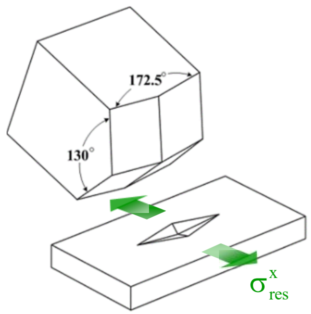

Stress-free Uni-axial stress

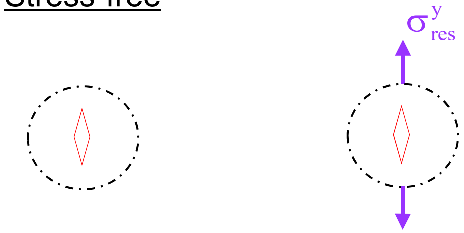

Comparison of indentation curves

$$\Delta L \approx \alpha_{//} \sigma^y_{res}$$

conversion factor in **parallel** direction

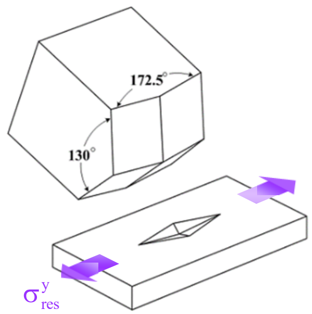

Separation of load difference with stress directions

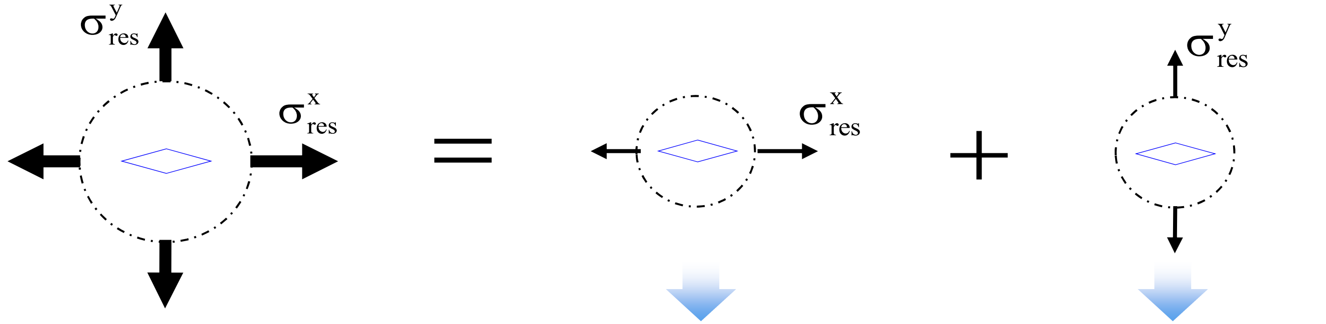

$$\Delta L_{//} = \alpha_{//}\sigma^{x}_{res} \qquad \Delta L_{\perp} = \alpha_{\perp}\sigma^{y}_{res}$$

$$\Delta L_2 = \Delta L_{//} + \Delta L_{\perp}$$

$$= \alpha_{//}\sigma^{x}_{res} + \alpha_{\perp}\sigma^{y}_{res}$$

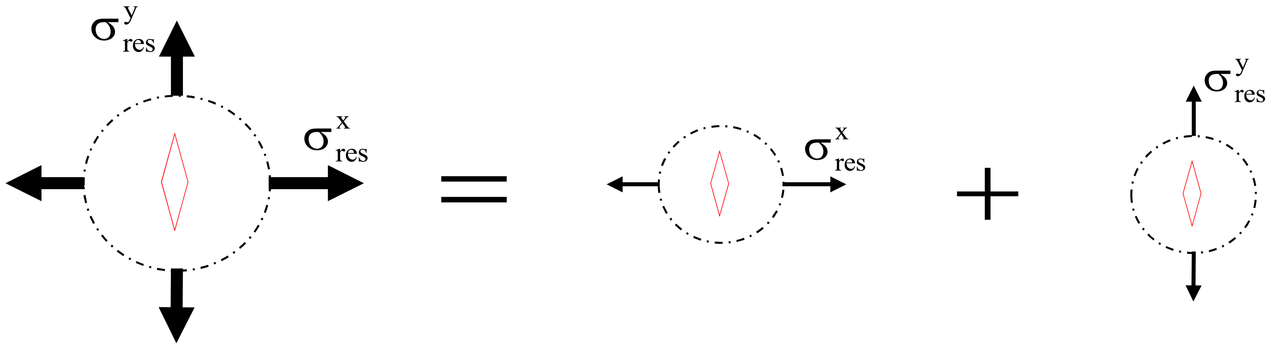

$$\Delta L_1 = \alpha_{\perp}\sigma^{x}_{res} + \alpha_{//}\sigma^{y}_{res}$$

Material Reliability
& Forensic Safety Lab.

Evaluation of Residual Stresses Directionality

$$\frac{\Delta L_2}{\Delta L_1} = \frac{\alpha_{//}\sigma^x_{res} + \alpha_{\perp}\sigma^y_{res}}{\alpha_{\perp}\sigma^x_{res} + \alpha_{//}\sigma^y_{res}} \Rightarrow \frac{\dfrac{\alpha_{//}}{\alpha_{\perp}} + \dfrac{\sigma^y_{res}}{\sigma^x_{res}}}{1 + \dfrac{\alpha_{//}}{\alpha_{\perp}}\dfrac{\sigma^y_{res}}{\sigma^x_{res}}} = \frac{\dfrac{\alpha_{//}}{\alpha_{\perp}} + p}{1 + \dfrac{\alpha_{//}}{\alpha_{\perp}} p}$$

$$\frac{\Delta L_2}{\Delta L_1} = \frac{\dfrac{\alpha_{//}}{\alpha_{\perp}} + p}{1 + \dfrac{\alpha_{//}}{\alpha_{\perp}} p} \Rightarrow p = \frac{\sigma^y_{res}}{\sigma^x_{res}} = \frac{\dfrac{\Delta L_2}{\Delta L_1} - \dfrac{\alpha_{//}}{\alpha_{\perp}}}{1 - \dfrac{\alpha_{//}}{\alpha_{\perp}}\dfrac{\Delta L_2}{\Delta L_1}}$$

$$\frac{\alpha_{//}}{\alpha_{\perp}} \approx 0.34$$

Empirical constant

Separation of stress

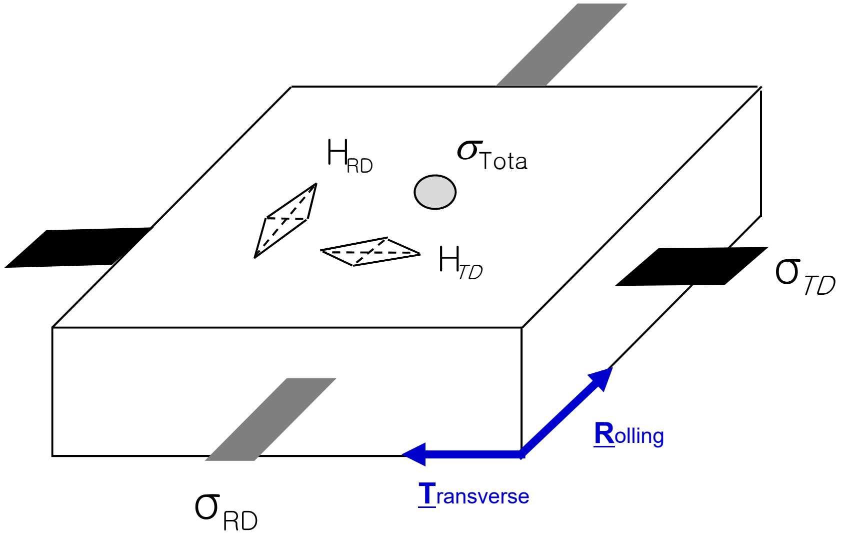

*Assumption

$$\sigma_{Total} = \frac{\sigma_{RD} + \sigma_{TD}}{2} = \frac{\sigma_{RD} + (p \cdot \sigma_{RD})}{2} \quad \left(p = \frac{\sigma_{RD}}{\sigma_{TD}}\right)$$

$$\sigma_{RD} = \frac{2 \cdot \sigma_{Total}}{(1+p)} \qquad \sigma_{TD} = 2 \cdot \sigma_{Total} - \sigma_{RD}$$

$$H_{RD} = \alpha_{TD}\sigma_{RD} + \alpha_{RD}\sigma_{TD}$$

$$H_{TD} = \alpha_{RD}\sigma_{RD} + \alpha_{TD}\sigma_{TD}$$

< *Invariant hardness* regardless of stress state >

$$\left(p = \frac{\sigma_{TD}}{\sigma_{RD}} = \frac{\frac{H_{TD}}{H_{RD}} - \frac{\alpha_{RD}}{\alpha_{TD}}}{1 - \frac{\alpha_{RD}}{\alpha_{TD}}\frac{H_{TD}}{H_{RD}}} \right)$$

Load-Depth difference according to indentation direction

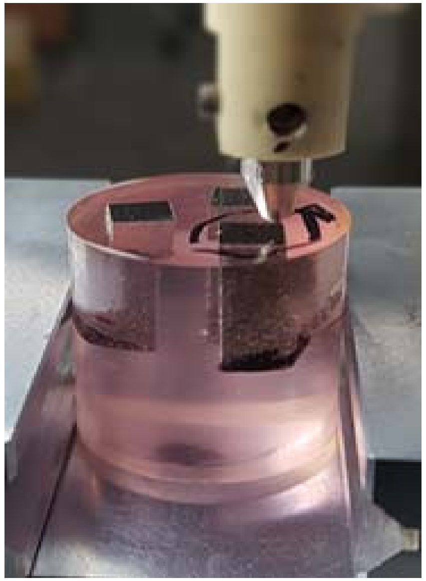

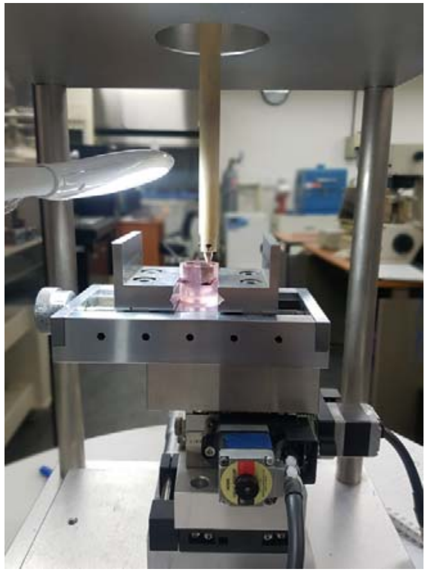

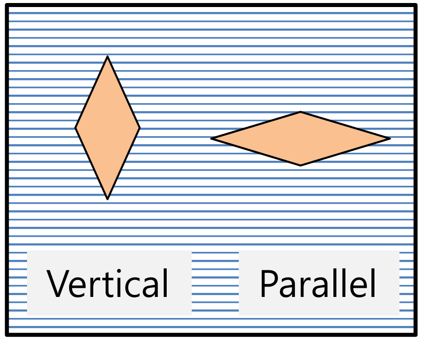

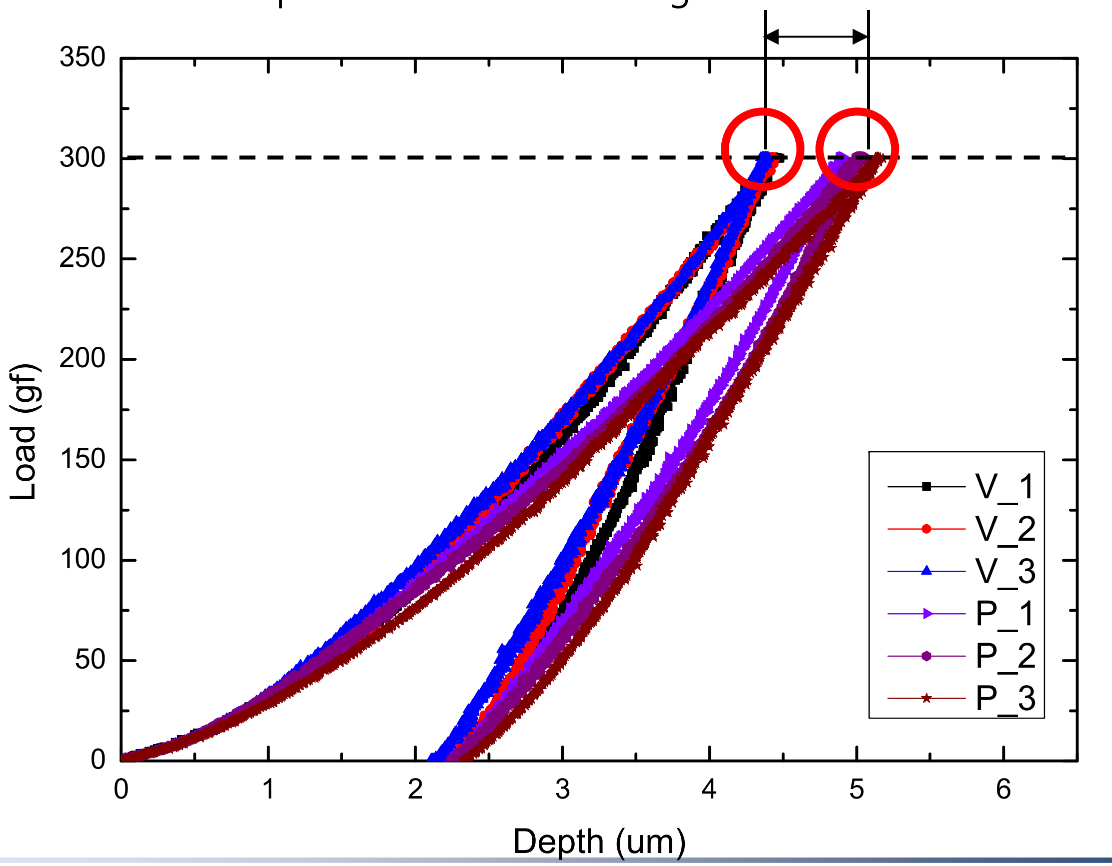

Anisotropy evaluation using DIC

* DIC

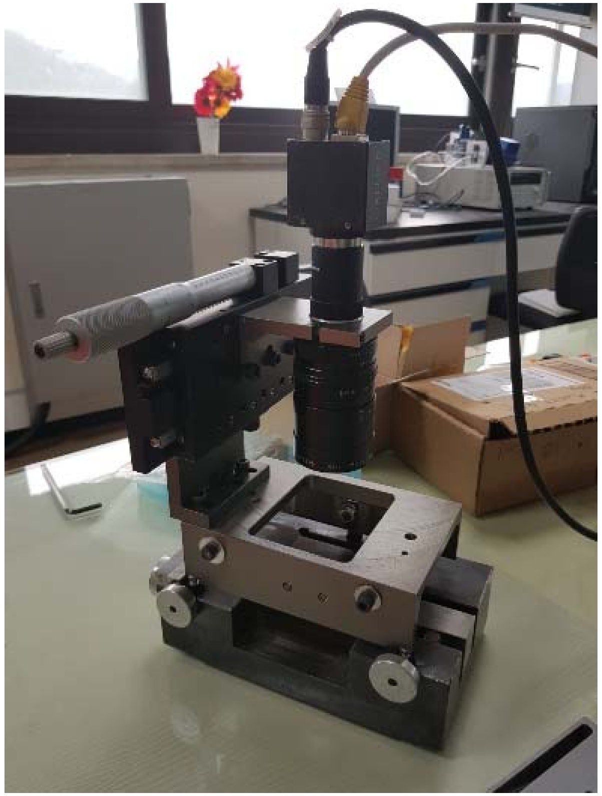

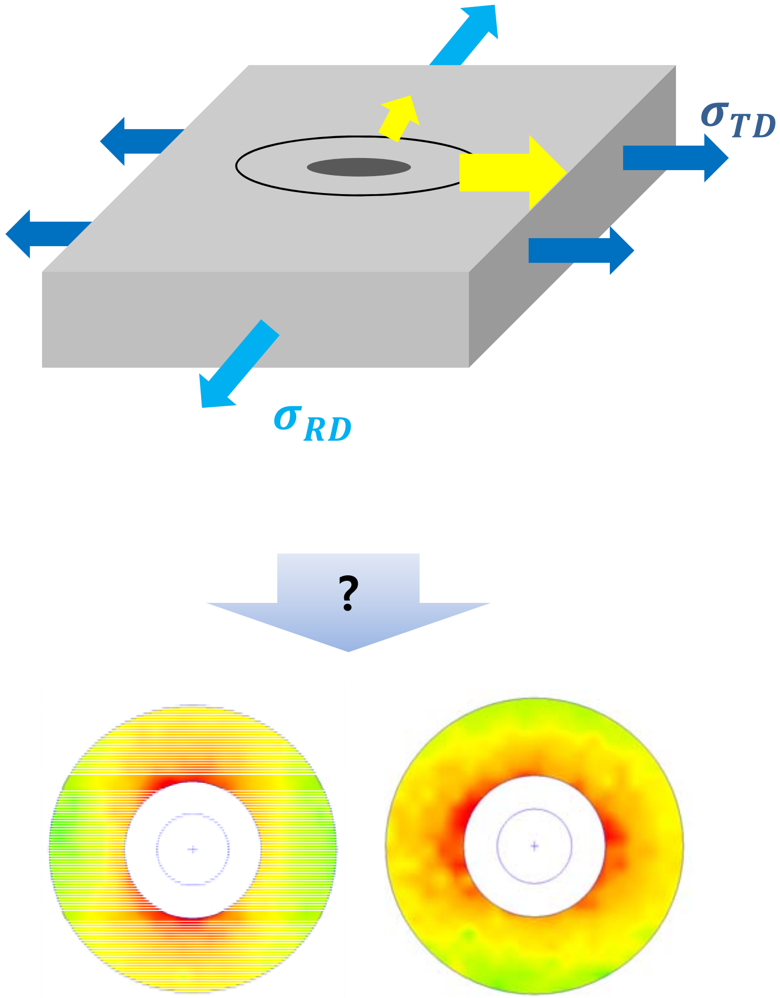

Future Paln

3D Printing material

Evaluation of anisotropy using IIT

Evaluation of anisotropy using DIC

Prediction of Anisotropy

Evaluation of anisotropy of amorphous materials by high energy X-ray scattering

Evaluation of amorphous anisotropy by measuring 4 point electrical resistance

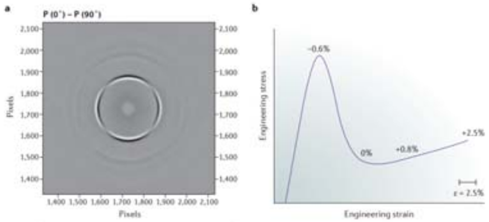

Figure 5 | **Anisotropy induced by homogeneous flow. a** | The difference between the diffraction pattern (P) of an anisotropic $Fe_{81}B_{13}Si_{4}C_{2}$ metallic-glass ribbon in two orthogonal orientations indicates that the first halo is elliptical[112]. The ribbon had undergone creep to a strain of 2–3% by loading in tension at 573 K for 30 minutes. The patterns were obtained in transmission with 87-keV X-rays. **b** | The stress–strain curve for a $Pd_{40}Cu_{30}Ni_{10}P_{20}$ bulk metallic glass under uniaxial compression[110] (strain rate 10^{-1} s^{-1}, 533 K). The labels show the percentage elastic anisotropy (defined as $(\mu_4 - \mu_6)/\mu_4$ for shear moduli μ_4 (≡C_{2323}) and μ_6 (≡C_{1212}) relative to the creep axis x_1 and transverse plane $x_2 - x_3$) measured by resonant ultrasound spectroscopy at room temperature for samples crept to the given points on the curve (that is, to approximate total inelastic strains of up to 30%). Panel **a** is adapted with permission from REF. 112, Wiley-VCH. Panel **b** is adapted with permission from REF. 110, Elsevier.

Validation of applying the model to 3D printing material


Thank You
for Your Attention